

Thermoelastic Analysis of Graphene-Based Nanomaterials

Stelios K. Georgantzinis¹, Georgios I. Giannopoulos² and Nick K. Anifantis³

Abstract

A numerical model for the prediction of the thermomechanical behavior of graphene-based nanomaterials is developed. The nanomaterials are modelled according to their atomistic structure. The harmonic approximation is utilized for describing the interaction potential energies and their expressions as functions of temperature approached using assumptions based on molecular theory. The force field is simulated via suitable straight and torsional spring mechanical equivalents. Springs express the interatomic interactions and interconnect nodes placed on the atomic positions. By using appropriate boundary conditions, the graphene-based nanomaterials are properly loaded and their thermoelastic response is numerically predicted using finite element procedures. A complete parametric study with respect to the geometric characteristics of the nanomaterials is performed, and the

¹ Mechanics Lab, Division of Mathematics and Engineering Studies, Department of Military Science, Hellenic Army Academy, Vari 16673, Greece.

Machine Design Lab, Department of Mechanical and Aeronautics Engineering, University of Patras, 26500 Rio, Greece. E-mail: sgeor@mech.upatras.gr

² Department of Mechanical Engineering, Technological Educational Institute of Patras, Patras, Greece. E-mail: ggiannopoulos@teiwest.gr

³ Machine Design Lab, Department of Mechanical and Aeronautics Engineering, University of Patras, 26500 Rio, Greece. E-mail: nanif@mech.upatras.gr

temperature dependency of elastic Young's modulus is finally predicted. Comparisons with available published works found in the literature demonstrate the accuracy of the proposed method.

Keywords: Graphene; nanomaterials; coupled thermomechanics; molecular mechanics; finite element modelling

1 Introduction

Nanomaterials can be designed at the atomic level, lending more control over their properties, and making them better suited to their desired purpose. Concerning army applications, nanostructured materials can make lighter armor, and extremely strong building materials, while nanofiber based duds offer enhanced protection against projectiles. It becomes evident, that nanomaterials will play an important role concerning the future offensive and defensive military technology and could contribute in the protection of soldiers as well as in the improvement of their equipment. Furthermore, such a military nanotechnology could be successfully expanded and transferred from the army to the general community [1]. In order to efficiently design such applications, the development of computational tools able to predict the nanomaterials behavior is required.

The elastic mechanical properties such as Young's modulus of graphene and carbon nanotubes has been investigated using various Molecular Dynamics (MD) based techniques [2] and molecular mechanics based finite element approaches [3]. The use of simulations to predict the temperature dependence of the graphene based nanomaterials mechanical properties is a necessity, because of the difficulties involved in obtaining direct experimental measurements in different thermal environments. However, all the predictive tools so far available to simulate and design the stiffness of CNT-based composites are not based on

analytical formulas that would facilitate the work of the material scientist and engineer. The existing atomistic-continuum models describing the elastic properties of carbon nanotubes in closed form [4] have their bonds force constant formulated only for room temperature.

The mechanical behavior of graphene nanoribbons (GNRs) has been scarcely investigated, partly due to the difficulty in patterning a graphene based nanostructure below 20 nm. Making measurements by nanoindentation in an atomic force microscope (AFM), Lee *et al.* [5] have shown that graphene has a breaking strength 200 times greater than steel. These measurements have revealed a Young's modulus of 1.0 TPa and intrinsic strength of 130 GPa. Recently, Rasuli *et al.* [6] have studied the mechanical properties of a few-layer graphene cantilever and a GNR using AFM. They have measured an in-plane Young's modulus for the GNR 0.7 TPa. The difficulty in investigating the mechanical behavior of GNRs via experimental procedures may be overcome via the use of numerical simulations capable of modeling nanostructures independently of their size and dimensionality.

In this paper, the thermomechanical behavior of graphene-based nanomaterials is studied developing a finite element based numerical model. It adopts two noded, linear, spring finite elements of three translational degrees of freedom per node. The harmonic approximation is utilized for describing the interaction potential energies and their expressions as functions of temperature using assumptions based on molecular theory. Specifically, spring elements having specific translational stiffness along bond direction and zero stiffness in the other directions are used to interconnect bonded carbon atoms (C–C nanostructure) and thus simulate exclusively bond stretching interaction. Furthermore, springs elements of explicit translational stiffness in the three directions are adopted to interconnect opposite atoms of two linked bonds (C–C–C nanostructure) in such a way that efficient simulation of both bond angle bending and bond angle twisting interaction may be achieved simultaneously. The

proposed method leads to low computational cost since rotational degrees of freedom at each nodal position are absent. A complete parametric study with respect to the geometric characteristics of the nanomaterials is performed, and the temperature dependency of elastic Young's modulus is finally predicted. Comparisons with available published works found in the literature demonstrate the accuracy of the proposed method.

2 Geometry of graphene

One of the most popular nanostructure material is graphene. Graphene is the geometric basis of other significant carbon allotropes such as graphite, fullerenes, graphitic flakes, and carbon nanotubes. A representative form of the ideal geometric structure of graphene is illustrated in Figure 1.

The geometry can be defined using the vectors \mathbf{r}_1 and \mathbf{r}_2 , that

$$|\mathbf{r}_1| = |\mathbf{r}_2| = \sqrt{3}r_T,$$

where r_T is the length of a C-C bond at the temperature T . In a Cartesian coordinate system is valid that

$$\mathbf{r}_1 = r_T \begin{bmatrix} 3/2 & \sqrt{3}/2 \end{bmatrix}^T, \mathbf{r}_2 = r_T \begin{bmatrix} 3/2 & -\sqrt{3}/2 \end{bmatrix}^T.$$

The vectors connecting any atom to its nearest neighbors are

$$\boldsymbol{\delta}_1 = (\mathbf{r}_1 - 2\mathbf{r}_2)/3, \boldsymbol{\delta}_2 = (\mathbf{r}_2 - 2\mathbf{r}_1)/3, \boldsymbol{\delta}_3 = (\mathbf{r}_1 + \mathbf{r}_2)/3.$$

The thermal dependence of the bond length, and consequently, of a graphene based nanomaterial is provided through an equivalent coefficient of thermal expansion (CTE) α , and is

$$r_T = r_0 (1 + \alpha \Delta T),$$

where $\Delta T = T - T_0$, T is the temperature of the environment, T_0 is the room temperature, and r_0 is the bond length at room temperature.

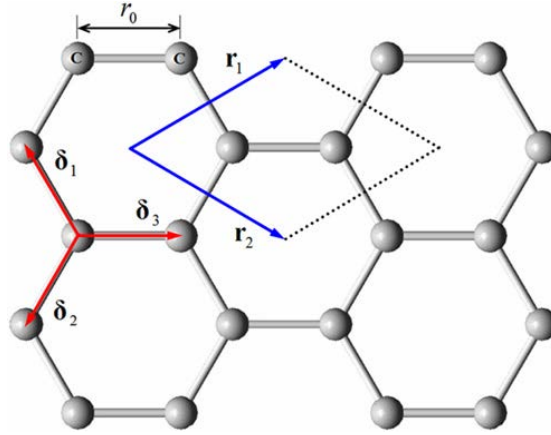


Figure 1: Ideal geometry of grapheme

3 Governing Equation

The total potential energy within graphene based nanostructures due to interatomic interactions by assuming small strains and adopting the simplest harmonic forms is given by the following equation

$$U = \sum U_r + \sum U_\theta + \sum U_\tau$$

where U_r represents the energy due to bond stretching, U_θ the energy due to bond angle bending and U_τ the energy due to dihedral angle torsion plus out-of-plane torsion. The above energies are given by the following equations, correspondingly

$$U_r = \frac{1}{2} k_r^T (\Delta r)^2, U_\theta = \frac{1}{2} k_\theta^T (\Delta \theta)^2, U_\tau = \frac{1}{2} k_\tau^T (\Delta \phi)^2$$

where k_r^T , k_θ^T and k_τ^T are the bond stretching, bond angle bending, bond angle twisting force constants that are functions of the temperature T , respectively, and Δr , $\Delta \theta$ and $\Delta \phi$ represent the bond length, bond angle bending and bond angle twisting variations, respectively.

Adopting partially the nomenclature of the Universal Force Field (UFF), the bond stretching constant is expressed as

$$k_r^T = 664.12 \frac{Z_i^* Z_j^*}{r_T^3}$$

where Z_i^* and Z_j^* are the effective electronic charges (1.914 electron units) of two neighboring atoms i and j , respectively. By using the above equation and taken that r_T is equal to 0.142 nm that at room temperature, the bond stretching coefficient becomes 6.52×10^{-7} N/nm, which is in agreement with the room temperature value obtained by the AMBER model. The bond angle constant k_θ^T actually is the second partial derivative of the bending energy functional

$$k_\theta^T = \left(\frac{\partial^2 U_\theta}{\partial \theta^2} \right) = \frac{\bar{\beta} Z_i^* Z_k^*}{r_{ik}^5} r_T r_T \{ 3 r_T r_T [1 - (\cos \theta)^2] - r_{ik}^2 \cos \theta \}$$

where r_{ik} is the distance between two adjacent atoms i and k in a C-C-C nanostructure. The distance between the atoms i and k is defined by

$$r_{ik} = r_T^2 + r_T^2 - 2 r_T r_T \cos \theta.$$

At room temperature the angle between the bonds is $\theta = 120^\circ$. The term $\bar{\beta}$ is equal to $336/r_T$, and therefore k_θ^T takes a value equal to 8.76×10^{-10} Nnm/rad² which is again consistent with the AMBER model.

The torsional potential energy is calculated approximately by the summation of three cosine Fourier terms based on the angle of a bond in a torsional deformation ω

$$U_\tau = k_\tau^T \sum_{n=0}^2 C_n \cos n\omega.$$

At room temperature the constant K_τ^0 is equal to 2.78×10^{-10} N/nm/rad². Due to the low dependency of the torsional constant in the temperature, we assume that is constant for all the temperature range (0 to 1600⁰K) that is studied here.

4 Finite element representation

In order to create an efficient finite element model some assumptions are adopted. As Figure 2 presents, the deformations of a C-C-C nanostructure could be represented by a set of linear springs. Observing Figure 2(a), someone may assume that the potential energy of the bond in stretching can be simulated by a linear spring, the strain energy of which is equal to the potential energy, i.e.

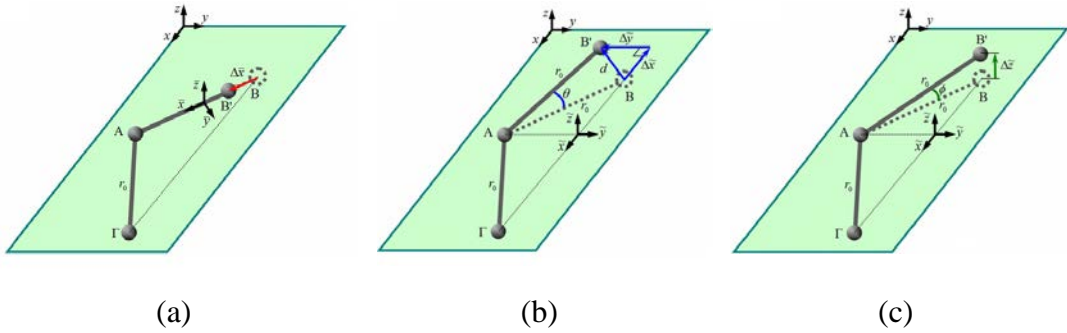


Figure 2: Interatomic deformations: (a) bond stretching, (b) bond angle bending and (c) bond angle twisting

$$U_r = \frac{1}{2} k_r^T (\Delta \bar{x})^2$$

where $\Delta \bar{x}$ is the translation of B in the longitudinal \bar{x} -axis of the spring. In Figure 2(b), for small deformations there is $\Delta \theta = d/r_0$ or

$$\Delta \theta = \frac{\sqrt{(\Delta \bar{x})^2 + (\Delta \bar{y})^2}}{r_0}.$$

Using the above equation, the potential energy of the bond angle bending interaction can be written as

$$U_\theta = \frac{1}{2} \frac{k_\theta^T}{r_0^2} (\Delta \bar{x})^2 + \frac{1}{2} \frac{k_\theta^T}{r_0^2} (\Delta \bar{y})^2.$$

Correspondingly, for small deformations, it can be assumed in Figure 2(c) that $\Delta \omega = \Delta \bar{z}/r_0$. Therefore, the potential energy of the bond torsion interaction can be written as

$$U_\varphi = \frac{1}{2} \frac{k_t^T}{r_0^2} (\Delta \bar{z})^2.$$

According to the aforementioned potential terms, the governing equation of a GNR system, which consists of numerous C–C nanostructures, may be written as

$$U = \sum \frac{1}{2} k_r^T (\Delta \bar{x})^2 + \sum \frac{1}{2} \frac{k_\theta^T}{r_0^2} (\Delta \bar{x})^2 + \sum \frac{1}{2} \frac{k_\theta^T}{r_0^2} (\Delta \bar{y})^2 + \sum \frac{1}{2} \frac{k_t^T}{r_0^2} (\Delta \bar{z})^2.$$

In order to represent the potential terms, two-noded spring elements of specific local coordinate systems, with six degrees of freedom per node i.e., three translations, are utilized.

Firstly, spring elements, called hereafter *cc*, are utilized for the simulation of bond stretching interaction. Applying the conventional displacement formulation, their equilibrium equation in their three dimensional local coordinate system $(\bar{x}, \bar{y}, \bar{z})$ can be written as

$$\mathbf{K}_{xyz}^{cc} \mathbf{u}_{xyz}^{cc} = \mathbf{f}_{xyz}^{cc},$$

where \mathbf{K}_{xyz}^{cc} denotes the displacement element stiffness matrix, \mathbf{u}_{xyz}^{cc} the generalized element displacement vector and \mathbf{f}_{xyz}^{cc} the generalized element force vector. The element displacement stiffness matrix, generalized displacement and force vectors, respectively, are

$$\mathbf{K}_{xyz}^{cc} = \begin{bmatrix} \mathbf{k}_{xyz}^{cc} & -\mathbf{k}_{xyz}^{cc} \\ -\mathbf{k}_{xyz}^{cc} & \mathbf{k}_{xyz}^{cc} \end{bmatrix},$$

$$\mathbf{u}_{xyz}^{cc} = [\mathbf{u}_{\bar{x}o}^{cc} \quad \mathbf{u}_{\bar{y}o}^{cc} \quad \mathbf{u}_{\bar{z}o}^{cc} \quad \mathbf{u}_{\bar{x}i}^{cc} \quad \mathbf{u}_{\bar{y}i}^{cc} \quad \mathbf{u}_{\bar{z}i}^{cc}]^T,$$

$$\mathbf{f}_{xyz}^{cc} = [\mathbf{f}_{\bar{x}o}^{cc} \quad \mathbf{f}_{\bar{y}o}^{cc} \quad \mathbf{f}_{\bar{z}o}^{cc} \quad \mathbf{f}_{\bar{x}i}^{cc} \quad \mathbf{f}_{\bar{y}i}^{cc} \quad \mathbf{f}_{\bar{z}i}^{cc}]^T.$$

where *o* and *i* are the two nodes of element *cc* and

$$\mathbf{k}_{xyz}^{cc} = \begin{bmatrix} k_r^T & 0 & 0 \\ 0 & 0 & 0 \\ 0 & 0 & 0 \end{bmatrix}.$$

Secondly, spring elements, called hereafter *ccc*, are utilized for the simulation of both bond angle bending and twisting interactions. Their equilibrium equation in their three dimensional local coordinate system $(\bar{x}, \bar{y}, \bar{z})$ is

$$\mathbf{K}_{\bar{x}\bar{y}\bar{z}}^{\text{ccc}} \mathbf{u}_{\bar{x}\bar{y}\bar{z}}^{\text{ccc}} = \mathbf{f}_{\bar{x}\bar{y}\bar{z}}^{\text{ccc}}$$

where $\mathbf{K}_{\bar{x}\bar{y}\bar{z}}^{\text{ccc}}$ denotes the displacement element stiffness matrix, $\mathbf{u}_{\bar{x}\bar{y}\bar{z}}^{\text{ccc}}$ the generalized element displacement vector and $\mathbf{f}_{\bar{x}\bar{y}\bar{z}}^{\text{ccc}}$ the generalized element force vector. The element displacement stiffness matrix, generalized displacement and force vectors, respectively, are

$$\mathbf{K}_{\bar{x}\bar{y}\bar{z}}^{\text{ccc}} = \begin{bmatrix} \mathbf{k}_{\bar{x}\bar{y}\bar{z}}^{\text{ccc}} & -\mathbf{k}_{\bar{x}\bar{y}\bar{z}}^{\text{ccc}} \\ -\mathbf{k}_{\bar{x}\bar{y}\bar{z}}^{\text{ccc}} & \mathbf{k}_{\bar{x}\bar{y}\bar{z}}^{\text{ccc}} \end{bmatrix},$$

$$\mathbf{u}_{\bar{x}\bar{y}\bar{z}}^{\text{ccc}} = \left[\mathbf{u}_{\bar{x}i}^{\text{ccc}} \quad \mathbf{u}_{\bar{y}i}^{\text{ccc}} \quad \mathbf{u}_{\bar{z}i}^{\text{ccc}} \quad \mathbf{u}_{\bar{x}j}^{\text{ccc}} \quad \mathbf{u}_{\bar{y}j}^{\text{ccc}} \quad \mathbf{u}_{\bar{z}j}^{\text{ccc}} \right]^T,$$

$$\mathbf{f}_{\bar{x}\bar{y}\bar{z}}^{\text{ccc}} = \left[\mathbf{f}_{\bar{x}i}^{\text{ccc}} \quad \mathbf{f}_{\bar{y}i}^{\text{ccc}} \quad \mathbf{f}_{\bar{z}i}^{\text{ccc}} \quad \mathbf{f}_{\bar{x}j}^{\text{ccc}} \quad \mathbf{f}_{\bar{y}j}^{\text{ccc}} \quad \mathbf{f}_{\bar{z}j}^{\text{ccc}} \right]^T.$$

where i and j are the two nodes of element *ccc* and

$$\mathbf{k}_{\bar{x}\bar{y}\bar{z}}^{\text{ccc}} = \frac{1}{r_{\bar{T}}^2} \begin{bmatrix} k_{\theta}^T & 0 & 0 \\ 0 & k_{\theta}^T & 0 \\ 0 & 0 & k_{\tau}^T \end{bmatrix}$$

In order to predict the elastic thermomechanical properties of GNRs, a linear static analysis should take place. Thus, the system of linear equations is constructed by applying the above mentioned elemental stiffness matrices for every *cc* and *ccc* element of the GNR and transformed to the global coordinate system (x,y,z) . Then all linear equations are assembled according to the requirements of nodal equilibrium and the following system of equations is obtained

$$\mathbf{K}\mathbf{U}=\mathbf{F}$$

where \mathbf{K} , \mathbf{U} and \mathbf{F} are the assembled stiffness matrix, displacement vector and force vector, respectively, of the nanostructure. This matrix equation can be solved via standard numerical techniques such as Gauss elimination or LU decomposition

by taking into consideration the imposed boundary condition. A representative model and the boundary conditions for the evaluation of elastic modulus is depicted in Figure 3.

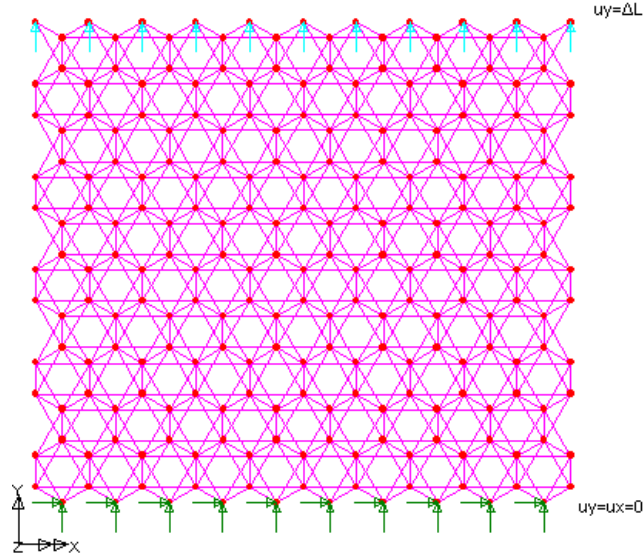


Figure 3: Boundary conditions on a FE model for the prediction of elastic modulus at a specific temperature

5 Results and Discussion

In order to compute Young's modulus of the graphene, a nodal uniform displacement u has been applied along the axis of loading at each node that belongs to the upper edge (see, Figure 3). Then, Young's modulus E of the graphene at a specific temperature has been computed from the following equation:

$$E = \frac{\sigma}{\varepsilon} = \frac{\frac{\sum_{p_1=1}^{q_1} (-p_1 f_1)}{wt}}{\frac{\Delta l}{l}}$$

where f_y^i is the reaction along axis of loading of node i and q is the total number of nodes that belong in the lower constrained edge of the graphene.

Due to the lack of similar detailed and parametrically investigated size dependent results, available in the literature, the attempted comparisons are focused on average estimations at room temperature. Table 1 includes some qualitative comparisons of average predicted Young's modulus E with corresponding average predictions from the literature. Good agreement can be observed between the present estimations and the other ones from theoretical [3,7,8] and experimental investigations [5,6].

Table 1: Comparison between the present method and other available approximations

| Study | t (nm) | E (TPa) |
|--------------------|---------------------------------------|-----------|
| Theoretical | Present method | 0.34 |
| | Continuum mechanics [7] | 0.34 |
| | Molecular Dynamics [8] | 0.34 |
| | Spring based structural mechanics [3] | 0.34 |
| Experimental | AFM [6] | — |
| | AFM [5] | 1.00 |

Since the method is validated, the next step is to utilize it in order to investigate the behaviour of the elastic properties of graphene at various temperatures. Figure 4, depicts the variation of Young's modulus E_y versus temperature for various graphene configurations. Note in Figure 3 that y-axis is parallel to the armchair edges and vertical to the zigzag edges of graphene. Figure 4 shows that all graphene configurations present the same behaviour as the temperature increases. The highest value of Young's modulus is observed around the room temperature (300°K). For temperatures higher than 300°K, a decrease of the elastic modulus is

observed. Moreover, the elastic modulus seems to decrease for temperatures lower to the room one, however, an increase is observed near the absolute temperature.

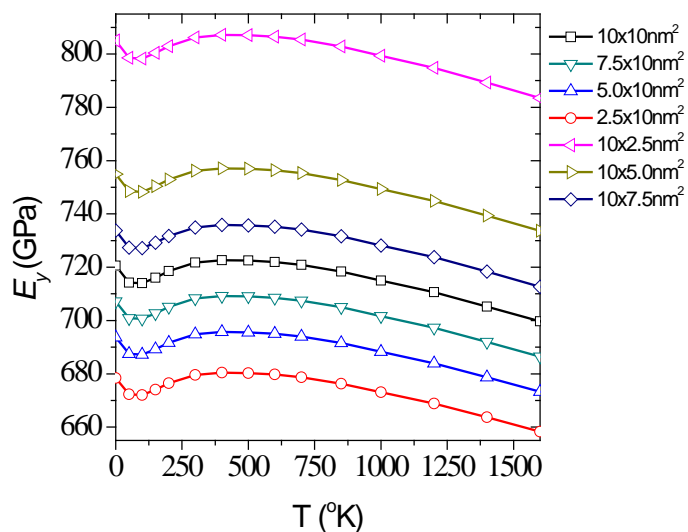


Figure 4: Young's modulus of graphene versus temperature concerning the zigzag direction

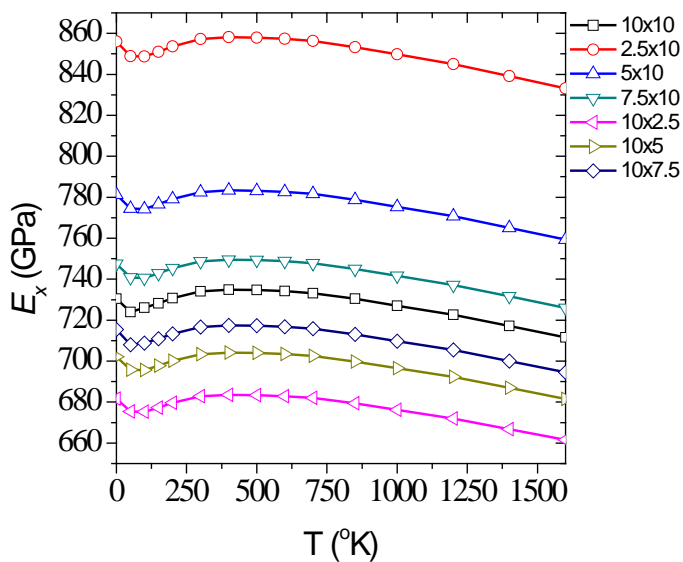


Figure 5: Young's modulus of graphene versus temperature concerning the armchair direction

Similarly, Figure 5 illustrate the results concerning elastic modulus obtained by investigating graphene behavior along x -direction. The revealed variation of elastic modulus along x -axis (armchair edges loaded) is similar with the one observed when zigzag edges are stretched. However, the elastic modulus is higher in this case, for all geometries considered. The highest value of the elastic modulus is around 860 GPa and is taken near the room temperature and for the 2.5nm \times 10nm configuration.

6 Conclusions

A structural mechanics method based on the use of straight spring elements of three degrees of freedom per node has been developed for the simulation of the linear thermoelastic behavior of graphene based nanomaterials at the temperature range from 0°K to 1600 °K. The advantage of the proposed method is its accuracy, simplicity and its low computational cost. Furthermore, it may as well be utilized for the simulation of thermoelastic mechanical response of single-walled carbon nanotubes and fullerenes.

Using the proposed method the above general findings for the thermoelastic behavior of graphene have been arisen:

- Graphene presents size-dependend mechanical properties at all temperature levels.
- The highest elastic modulus is presented around the room temperature.
- Armchair direction presents higher values of elastic modulus for all temperature values.

References

- [1] D. Moore, *Nanotechnology and the military, Nanoethics: The Ethical and Social Implications of Nanotechnology*, pod redakcją F. Allhoff, P. Lin, J. Moor, J. Weckert, pub. John Wiley & Sons, (2007), 267.
- [2] C.L. Zhang, H.S. Shen, Temperature-dependent elastic properties of single-walled carbon nanotubes: Prediction from molecular dynamics simulation, *Applied Physics Letters*, **89**, (2006), 081904.
- [3] S.K. Georgantzinou, G.I. Giannopoulos, D.E. Katsareas, P.A. Kakavas and N.K. Anifantis, Size-dependent non-linear mechanical properties of graphene nanoribbons, *Computational Materials Science*, **50**(7), (2011), 2057–2062.
- [4] T. Chang and H. Gao, Size-dependent elastic properties of a single-walled carbon nanotube via a molecular mechanics model, *Journal of the Mechanics and Physics of Solids*, **51**(6), (2003), 1059–1074.
- [5] C. Lee, X. Wei, J. W. Kysar and J. Hone, Measurement of the Elastic Properties and Intrinsic Strength of Monolayer Graphene, *Science*, **321**(5887), (2008), 385-388.
- [6] R. Rasuli, A. Irajizad and M.M. Ahadian, Mechanical properties of graphene cantilever from atomic force microscopy and density functional theory, *Nanotechnology*, **21**(18), (2010), 185503
- [7] M. Arroyo and T. Belytschko, Finite crystal elasticity of carbon nanotubes based on the exponential Cauchy-Born rule, *Physical Review B*, **69**, (2004), 115415.
- [8] Z. Xu, Graphene nano-ribbons under tension, *Journal of Computational and Theoretical Nanoscience*, **6**(3), (2009), 625-628.